



Published in final edited form as:

*J Am Chem Soc.* 2012 June 27; 134(25): 10664–10669. doi:10.1021/ja303737a.

## ***In-vivo* Fluorescence Imaging in the NIR-II with Long Circulating Carbon Nanotubes Capable of Ultra-High Tumor Uptake**

Joshua T. Robinson<sup>‡</sup>, Guosong Hong<sup>‡</sup>, Yongye Liang, Bo Zhang, Omar K. Yaghi, and Hongjie Dai<sup>\*</sup>

The Department of Chemistry, Stanford University, Stanford, California 94305

### **Abstract**

Cancer imaging requires selective high accumulation of contrast agents in the tumor region and correspondingly low uptake in healthy tissues. Here, by making use of a novel synthetic polymer to solubilize single-walled carbon nanotubes (SWNTs), we prepared a well-functionalized SWNT formulation with long blood circulation (half life ~ 30 h) *in vivo* to achieve ultra-high accumulation of ~30% injected dose (ID)/gram in 4T1 murine breast tumors in Balb/c mice. Functionalization dependent blood circulation and tumor uptake was investigated through comparisons with phospholipid-PEG solubilized SWNTs. For the first time, we performed video-rate imaging of tumors based on the intrinsic fluorescence of SWNTs in the second near infrared (NIR-II, 1.1–1.4  $\mu\text{m}$ ) window. We carried out dynamic contrast imaging through principal component analysis (PCA) to immediately pinpoint the tumor within ~20 s post injection. Imaging over time revealed increasing tumor contrast up to 72 h post injection, allowing for its unambiguous identification. 3D reconstruction of the SWNTs distribution based on their stable photoluminescence inside the tumor revealed a high degree of colocalization of SWNTs and blood vessels, suggesting enhanced permeability and retention (EPR) effect as the main cause of high passive tumor uptake of the nanotubes.

### **Keywords**

Carbon Nanotubes; Fluorescence; Principal Component Analysis; Tumor Accumulation

## **INTRODUCTION**

The field of nanomedicine has grown rapidly in recent years.<sup>1,2</sup> Nanoparticles have been used to enhance traditional medicine in the area of disease detection, prevention and treatment.<sup>3–5</sup> *In vivo* tumor imaging represents one of the areas where nanotechnology has shown promising results. Single-walled carbon nanotubes (SWNTs) exhibit intrinsic photoluminescence (PL) in the near-infrared (NIR) light region, known as the desirable

<sup>\*</sup>Corresponding Author. (hdai@stanford.edu).

<sup>‡</sup>These authors contributed equally.

### **ASSOCIATED CONTENT**

**Supporting Information.** Experimental details, further characterization of the SWNTs, and videos of the SWNTs in the mouse after injection and 3D reconstruction of a SWNT containing tumor are provided in the supporting information. This material is available free of charge via the Internet at <http://pubs.acs.org>.

Balb/c mice were purchased from Charles River and were housed at Stanford Research Animal Facility under Stanford Institutional Animal Care and Use Committee protocols.

### **Author Contributions**

The manuscript was written through contributions of all authors.

All authors have given approval to the final version of the manuscript.

'biological window' due to the low optical scattering,<sup>6,7</sup> absorption<sup>8</sup> and autofluorescence<sup>9,10</sup> by endogenous tissues in this range.<sup>9,11</sup> The large Stokes shift of 400–500 nm for SWNTs also allows for imaging with low background.<sup>12</sup> *In vivo* fluorescent imaging has inherent advantages due to its quick feedback and high spatial resolution.<sup>13</sup> Dynamic contrast-enhanced fluorescence imaging may also facilitate tumor imaging and differentiation of tumor from surrounding normal tissues and organs.<sup>11</sup> It is known that tumors behave differently from normal tissues with fenestration of blood vessels<sup>14,15</sup> inside tumors. Vessel imaging could serve as the basis for distinguishing tumor area from normal tissues.

The unique optical properties of SWNTs make them useful *in vivo* fluorescent imaging agents. Proper functionalization with amphiphilic surfactant imparts SWNTs with high biocompatibility, affording stealth particles that avoid rapid removal by the body's immune system.<sup>16,17</sup> SWNTs have been used for drug delivery,<sup>18</sup> photoacoustic imaging,<sup>19,20</sup> NIR photoluminescence imaging,<sup>21</sup> and photothermal therapy.<sup>17,22</sup> Properly functionalized SWNTs can afford high tumor uptake through the enhanced permeability and retention (EPR) effect even without targeting agents.<sup>23,24</sup> Here, using a relatively large 90 kilo-Dalton (kDa) amphiphilic poly(maleic anhydride-alt-1-octadecene)-methoxy poly(ethylene glycol) [C<sub>18</sub>-PMH-mPEG]<sup>25</sup> coating for nanotubes, we were able to achieve unprecedented 30% Injected Dose/gram tumor accumulation of SWNTs. Although a significantly higher molecular weight C<sub>18</sub>-PMH-mPEG has been previously used to coat SWNTs for long circulation time,<sup>16,17,22</sup> our current work has optimized the size of the starting C<sub>18</sub>-PMH to achieve one of the highest nanoparticle tumor accumulation levels to date. The 90 kDa C<sub>18</sub>-PMH-mPEG coated the SWNT non-covalently, which preserved the intrinsic NIR photoluminescence and strong Raman graphitic 'G' band of the SWNTs and allowed for *in vivo* imaging and *ex vivo* quantification of the pharmacokinetics. Other studies examined covalent functionalization of SWNTs. Oxidized SWNTs with carboxylic acids were linked to PEG and 1,3-dipolar cycloaddition was also used for PEGylation of SWNTs.<sup>26,27</sup> Covalently functionalized SWNTs were promising for cancer therapeutics delivery,<sup>28</sup> but diminished the intrinsic spectroscopic signatures of SWNTs for imaging and tracking.

We performed *ex vivo* imaging of tumor slices for 3D reconstruction of the tumor based on the intrinsic fluorescence of SWNTs in the second NIR region (1.1–1.4 μm), revealing the distribution of SWNTs inside the tumor and probing the degree of penetration of SWNTs inside the tumor. We also showed that high-frame-rate video imaging with dynamic contrast facilitated by principal component analysis (PCA) is a novel approach to distinguish tumor from normal tissues based on their different blood circulating behaviors. It has been reported that high-frame-rate video imaging based on the fluorescence of organic fluorophores and SWNTs can be combined with PCA to dynamically enhance the contrast of different normal organs and increase the anatomical resolution of mice.<sup>11,29</sup> Due to angiogenesis<sup>30</sup> during growth of tumor, which contains many newly born, fenestrated vessels,<sup>31</sup> blood flows differently in tumor than in normal tissues, making the tumor distinguishable from normal organs based on video imaging and PCA, as reported here for the first time.

## RESULTS AND DISCUSSION

To make water soluble and biocompatible SWNT suspension, we bath-sonicated HiPCO (Unidym) SWNTs in poly(maleic anhydride-alt-1-octadecene)methoxy(polyethyleneglycol) [C<sub>18</sub>-PMH-mPEG], a 90 kDa,<sup>25</sup> amphiphilic surfactant with ~9 repeating units (Fig. 1a, see methods for synthesis). Details of the preparation for individual, water soluble SWNTs can be found in the supplementary information. The UV-Vis-NIR absorption spectrum (Figure 1b) of the resulting SWNT suspension has multiple peaks corresponding to van Hove singularity transitions of different chiralities, suggesting a stable, well-suspended solution of

nanotubes. Figure 1c shows the photoluminescence versus excitation (PLE) spectrum of the SWNT suspension, where the four chiralities indicated by the arrows are the most likely ones to be excited by an 808 nm laser due to resonance. The photoluminescence quantum yield of the SWNTs used in this work was ~0.1% as the tube suspension was made by direct sonication in surfactant solutions.<sup>9</sup> An up to ~30-fold increase in quantum yield could be obtained by a surfactant exchange method.<sup>9</sup> A Raman scattering spectrum of the SWNTs upon excitation of 785 nm exhibited strong graphitic band (G band) resonance,<sup>26</sup> which is characteristic to graphitic carbon materials including SWNTs (Figure 1d).

A 200  $\mu$ L suspension of SWNT at a concentration of ~0.35 mg/mL (~3.5 mg/kg dose) was injected intravenously into a mouse with a subcutaneous xenograft 4T1 murine tumor located on the right hind limb. Video rate fluorescent images based on the intrinsic NIR-II fluorescence of SWNTs in the 1.1~1.4  $\mu$ m region upon excitation of 808 nm were taken continuously right after injection to track SWNT blood circulation in real time up to 210 s post injection (p.i.), as shown in Supplementary Movie 1. An exposure time of 100 ms enabled us to capture images at a frame rate of ~8 frame/sec (including an overhead time of ~18 ms in readout). Supplementary Movie 1 revealed the path of SWNTs through the body, showing blood circulating to the lungs and heart through the veins to be oxy-generated (Figure 2a) before being pumped into other organs including kidneys and liver through the artery (Figure 2b). Interestingly, besides the normal organs that were lit up by SWNT fluorescence, SWNT fluorescence in the 4T1 tumor started to appear at 8.0 s post injection (p.i.) and increased in intensity over time (Figure 2c). At 15.1 s p.i., major vessels inside the tumor showed up (Figure 2d). Clearer vascular structure in the tumor area could be identified from 20 s to 30 s p.i (Figure 2e). After 60 s p.i., tumor region could be distinguished from nearby normal tissues due to clear outline of the tumor (Figure 2f).

To gain further anatomical information of the tumor, PCA was applied to a time series of the first 200 fluorescence images (within 23.8 s p.i.). Previous work showed PCA as a powerful tool of discriminating organs based on their different blood circulating behaviors, since PCA turns pixels into groups (components) based on their variance, i.e., PCA groups pixels that vary similarly in time.<sup>11,29</sup> The pixel intensity in the tumor region differed from other organs as blood flowed later into the tumor than normal organs such as lungs, liver and kidneys, presumably due to the small size and random structure of newly born vessels. This difference, unique to tumors, allowed us to pick up the tumor as a single component from PCA, as shown in Figure 2g–2i. The positive pixel image in Figure 2g showed major vessels in the tumor color-coded in cyan, along with lungs and kidneys that could also be identified easily. The negative pixel image in Figure 2h showed the main body of the tumor, color-coded in chartreuse, which made the tumor a distinct component from all other organs. Moreover, the combined image in Figure 2i overlaid both positive and negative images and allowed us to visualize both the tumor outline (chartreuse) and vasculature inside the tumor (magenta). Interestingly, it was not until ~60 s p.i. (Figure 2f) that the tumor outline became distinguishable from nearby skin in the video, while all other organs were even brighter than the tumor. However, PCA analysis based on only the first frames within 23.8 s p.i. was able to delineate the tumor distinctly from all other normal tissues and organs, suggesting PCA as a useful tool for immediate tumor detection. We reproduced this finding on three other mice.

By collecting blood at various time points after injection and measuring the blood SWNT concentration using Raman spectroscopy,<sup>26</sup> we were able to extrapolate the blood circulation half-life of approximately 30 hours (Figure 3a). Due to the extremely long circulation of SWNTs and continuous accumulation of SWNTs in the tumor interstitial space owing to the enhanced permeability and retention (EPR) effect,<sup>32</sup> steady increase of NIR fluorescence in the tumor region was observed on all injected mice, as shown in the

time course NIR images taken on one of the mice (n=4) over a 72 hour time period (Figure 4a–d). To quantify the biodistribution of the SWNTs, mouse organs (n=4) were collected 100 hours post SWNT injection (See Methods).<sup>26</sup> There was no toxicity observed in the mice after the injection of SWNTs. Previous studies have investigated the long-term biodistribution, blood chemistry, and toxicity of SWNTs coated with phospholipid-PEG<sup>33</sup> and DSPE-mPEG/larger 1 MDa C<sub>18</sub>-PMH-mPEG.<sup>17</sup> In both studies, there was no indication of long-term toxicity. The clearance of the phospholipids-PEG SWNTs occurred primarily through the biliary pathway (feces) with a small portion of the SWNTs being excreted through renal filtration (urine).<sup>33</sup> The 30% injected dose/gram tumor uptake (Figure 3b) is one of the highest known tumor accumulations of intravenously injected nanoparticles ever observed, according to our survey of the literature. The tumor visibly darkened 72 hours post SWNT injection (Figure 4e), highlighting the significant accumulation in cancerous tissue. Previously, the highest reported tumor uptake of SWNTs was 23% ID/gram<sup>22</sup> which had high skin uptake of SWNTs, making it undesirable for imaging. Note that attaching targeting ligands to SWNTs could lead to further improvement of tumor uptake.<sup>34</sup>

The reduction in size of the C<sub>18</sub>-PMH-mPEG surfactant could be a contributing factor in the 80% reduction in skin accumulation of the SWNTs. It has been speculated that the larger, 1 MDa C<sub>18</sub>-PMH-mPEG coated SWNTs became trapped in the dermis due to their bulky size;<sup>22</sup> 90 kDa C<sub>18</sub>-PMH-mPEG SWNTs may avoid entrapment in the skin because of the smaller hydrodynamic radius. However, we do not have definitive proof as to why the smaller C<sub>18</sub>-PMH-mPEG SWNTs have lower skin uptake and this is an ongoing area of investigation.

We further examined the blood circulation behavior and tumor accumulation of SWNTs functionalized by several popular types of surfactants, including 1,2-distearoyl-phosphatidylethanolamine-methyl-poly(ethylene glycol) (DSPE-mPEG, 5 kDa) (Figure 3c). DSPE-mPEG coated SWNTs had circulation half-life of ~3.5 hours and tumor accumulation of 4% ID/gram. This data supports the assertion that long circulation time is necessary for high tumor uptake of nanoparticles. A particle with more passes through the fenestrated tumor vasculature increases the overall probability of tumor uptake.<sup>35,36</sup>

To reveal the spatial distribution of SWNTs accumulation, a tumor was collected and fixed for microtome slicing 100 hours after SWNT injection. The tumor, with volume ~ 20 mm<sup>3</sup>, yielded 50 slices each with ~40 μm thickness. Using rat anti-mouse CD31 and Cy5 labeled anti-rat IgG antibodies, we stained all tumor slices and imaged the location of the CD31 proteins, using the Cy5 emission at ~700 nm upon excitation at 658 nm. CD31 is commonly found at sites of angiogenesis,<sup>37</sup> and therefore anti-mouse CD31 has been widely used as an indicator of blood vessels. In our case rat anti-mouse CD31 bound to mouse CD31 in the blood vessels and a secondary antibody, Cy5 labeled anti-rat IgG bound to rat anti-mouse CD31 in order to visualize the distribution of CD31 for fluorescence imaging

For every slice we imaged the blood vessels stained by Cy5 and SWNT NIR-II fluorescence excited by the same 658 nm excitation. A 10× objective was used to block scan the whole slice (5 mm × 6 mm) with a step size of 200–500 μm. We then overlaid the blood vessels (color-coded in green) and SWNTs (color-coded in red) to assess colocalization (Fig. 5a). The overlaid image of a tumor slice revealed most of the SWNTs (in red and yellow regions) located at the peripheral area of the tumor. We did observe vascular structures deep inside the tumor color-coded in yellow due to SWNT colocalization with large vessel structures inside the tumor (Fig. 5a). We imaged all of the tumor slices of an entire tumor and then reconstructed the tumor in 3D using the ImageJ software (see Supplementary Movies 2, 3 and a snapshot in Figure 5b). Overall, a high degree of colocalization of SWNT and major vessels in the tumor was observed (abundant yellow colors, Figure 5b) while the

small vascular structures appeared impermeable to the SWNTs (green colors in Figure 5a&b).

## CONCLUSIONS

Achieving high tumor uptake of C<sub>18</sub>-PMH-mPEG (90 kDa) coated SWNTs after intravenous injection allowed for improved detection by NIR-II imaging. The accumulation of SWNTs inside the tumor steadily increased over 72 h p.i., owing to the extremely long circulation of nanotubes. The high tumor uptake could potentially be used to push the lower size limit of tumor detection and imaging. Colocalization analysis based on tumor slice imaging and 3D reconstruction revealed distribution of SWNTs mainly in the highly vascularized region and the edges of the tumor. Substantial extravasation of SWNTs was also observed. The combined high tumor accumulation ability and ideal fluorescence excitation/emission properties make SWNTs excellent candidates for nanomedicine.

## EXPERIMENTAL DETAILS

### Synthesis of C<sub>18</sub>-PMH-mPEG polymer

Octadecene (0.606 g, 2.4 mmol) and maleic anhydride (0.235 g, 2.4 mmol, freshly recrystallized from toluene) were added to a 10 mL flask, followed by the addition of 4 mL anhydrous dioxane. After all the solids were dissolved, azo bisisobutyronitrile (AIBN, 0.100 g, 0.60 mmol, freshly recrystallized from methanol) was added. The flask was installed with a condenser, and closed with a rubber stopper. The reaction system was vacuumed to remove air and then back filled with nitrogen. Such sequence was repeated for 3 times. The reaction system was heated to 100° C under nitrogen protection for 6 h. After the reaction cooled to room temperature, the solution was added dropwise to 50 mL cold methanol. The polymer was collected by centrifugation and re-precipitated from tetrahydrofuran (THF) into cold methanol. The polymer was collected by centrifuge and dried under vacuum for 1 day. The product was collected as a white solid (yield 70 %, Mn= 3.2kDa, PDI=1.1). Molecular weights and distributions of polymers were determined by using a Waters GPC liquid chromatograph equipped with a Waters 515 HPLC pump, a Waters 2414 refractive index detector, and a Waters 2489 UV/Visible detector. Polystyrene standards (Aldrich) were used for calibration, and THF was used as the eluent.

10 mg of the poly(maleic anhydride-alt-1-octadecene) product was added to 13.5 mL of dimethyl sulfoxide and 1.5 mL of pyridine. 285.7 mg of methoxy-terminated poly(ethylene glycol) amine (5 kDa MW) was then added to the solution which was stirred at room temperature for 12 h. Next, 22.7 mg of 1-Ethyl-3-(3-dimethylaminopropyl)carbodiimide (EDC) was added to the solution which continued to stir at room temperature for 24 h. The solution was dialyzed against water through dialyzing membrane (12–14 kDa MWCO) with 8× water changes to remove any unreacted methoxy-terminated poly(ethylene glycol) amine or poly(maleic anhydride-alt-1-octadecene). The resulting C<sub>18</sub>-PMH-mPEG product was then lyophilized and stored at –20° C until use.

In order to determine the degree of PEGylation of the C<sub>18</sub>-PMH-mPEG, we performed <sup>1</sup>H NMR in CDCl<sub>3</sub> (300 MHz). The peaks from 3.3–3.8 ppm (broad, CH<sub>2</sub> from mPEG) and 1.1–1.3 (CH<sub>2</sub> from the C<sub>18</sub> chain) were compared. The ratio was ~25–26:1, indicating that the C<sub>18</sub>-PMH precursor was fully PEGylated. <sup>1</sup>H NMR (300 MHz, CDCl<sub>3</sub>) δ: 3.3–3.8 (m, br, CH<sub>2</sub> of mPEG), 1.1–1.3 (m, CH<sub>2</sub> of C<sub>18</sub> chain), 0.88 (m, br, CH<sub>3</sub> of C<sub>18</sub>-PMH). In order to confirm that the C<sub>18</sub>-PMH-mPEG does not degrade during bath sonication, the surfactant was sonicated at a 1 mg/ml concentration for 1 hour, followed by 4× dialysis against water with a 12–14 kDa MWCO dialyzing membrane to remove any detached or degraded PEG chains. <sup>1</sup>H NMR in CDCl<sub>3</sub> (300 MHz) of the sonicated C<sub>18</sub>-PMH-mPEG showed a similar

spectrum, with the peaks from 3.3–3.8 ppm (broad, CH<sub>2</sub> from mPEG) and 1.1–1.3 (CH<sub>2</sub> from the C<sub>18</sub> chain) having a 24:1 ratio, indicating that the C<sub>18</sub>-PMH-mPEG remains intact after sonication.

### Preparation of biocompatible SWNTs

0.2 mg/mL HiPCO SWNTs (Unidym) and 1 mg/mL 90 kDa C<sub>18</sub>-PMH-mPEG were added to 10 mL of deionized ultra-filtered (DIUF) water and bath sonicated for 1 h. Following sonication, 2.5 mL of 10× phosphate buffered saline (PBS) was added to the solution. The SWNT suspension was then centrifuged at 22,000g for 6 hours to remove any aggregates and uncoated nanotubes. The supernatant was then collected and analyzed by atomic force microscopy to ensure that only individual SWNTs remained (data not shown). The SWNT solution was then washed 8 times by centrifuge filtration in DIUF water with a 100 kDa MWCO (Millipore) to remove any excess polymer though some excess polymer remained in solution after washing. The final SWNT solution was concentrated down in 2× Phosphate Buffer Saline (PBS) using the 100 kDa MWCO centrifuge filter and centrifugation at 4000g for 15 minutes. The concentrated SWNT remains above the membrane filter. 2× Phosphate Buffer Saline is used to mimic the pH and salt concentration found in the blood; any intravenous injection needs to be in 2× PBS in order not to harm the mouse by rapidly shifting the buffer and pH of the blood. The SWNT concentration was brought to 0.35 mg/ml as determined by UV-Vis-NIR spectroscopy (Cary 6000i) based on a mass extinction coefficient of SWNTs of 46.5 L/(g•cm) at 808 nm.<sup>17</sup>

To determine the degree of surfactant functionalization of the SWNTs, we lyophilized 1 ml of 0.5 mg/ml SWNT solution and weighed the resulting solid. The weight was 4.33 mg, indicating that there was approximately a 7.66:1 weight ratio of 90 kDa C<sub>18</sub>-PMH-mPEG surfactant:SWNT. This was equivalent to 9.67 C<sub>18</sub>-PMH-mPEG molecules/100 nm of SWNT.

For DSPE-mPEG SWNT, 0.2 mg/ml HiPCO SWNTs (Unidym) and 1 mg/ml 1,2-Distearoyl-phosphatidyl ethanolamine-methyl-polyethyleneglycol (DSPE-mPEG, 5 kDa, Laysan Bio Inc.) were added to 10 ml of deionized ultra-filtered (DIUF) water and bath sonicated for 1 h. SWNTs were then centrifuged and washed in the same manner as the C<sub>18</sub>-PMH-mPEG SWNT.

For 1–2 MDa C<sub>18</sub>-PMH-mPEG SWNT, 0.2 mg/ml HiPCO SWNTs (Unidym) and 1 mg/ml 1 MDa C<sub>18</sub>-PMH-mPEG were added to 10 ml of deionized ultra-filtered (DIUF) water and bath sonicated for 1 h. SWNTs were then centrifuged and washed in the same manner as the 90 kDa C<sub>18</sub>-PMH-mPEG coated SWNTS.

Dynamic Light Scattering (DLS) was used to determine the hydrodynamic radius of the SWNT solutions using a Brookhaven Instruments 90Plus Particle Size analyzer and a 1 cm quartz cuvette. A 0.05 mg/ml concentration of SWNT in water was used for all DLS measurements.

Atomic Force Microscopy (AFM) was used to show the size of 90 kDa C<sub>18</sub>-PMH-mPEG coated SWNTS as well as demonstrate the coating on the SWNTs. To prepare the SWNTs for AFM, 50 µL of a 0.05 mg/ml SWNT solution was placed on 1 cm silicon substrate for 20 minutes that was pre-soaked in 3-Aminopropyltriethoxysilane (APTES).

### Mouse Injection and Handling

BALB/c mice (n=4) were purchased from Charles River and were housed at Stanford Research Animal Facility under Stanford Institutional Animal Care and Use Committee protocols. When they reached 8 weeks in age, mice were inoculated with 1 million 4T1 cells

(ATCC #: CRL-2539) on the right hind limb. Tumors were allowed to grow for 7 days, at which point they were ~20–50 mm<sup>3</sup> in volume. The tumor size was monitored with digital calipers. On day 7, 200 µL of 0.35 mg/mL SWNT solution in 2× PBS buffer was injected intravenously through the tail, and video-rate imaging was taken during and after injection. The mice did not experience any weight loss or change in behaviour after injection. To anesthetize the mice for injection and subsequent imaging, the mice were placed in a knockdown box which had 2 L/min O<sub>2</sub> with 2.5% isoflurane flow through.

### Video-rate NIR imaging

Video-rate NIR imaging was carried out on a homebuilt setup consisting of a 2D InGaAs camera (Princeton Instruments). The geometry of the imaging setup can be found in our previous publication. The excitation light was provided by a fiber-coupled 808-nm diode laser (RMPC Lasers), chosen to overlap with the traditional biological transparency window and thus to afford maximum penetration. The light was collimated by a 4.5-mm focal length collimator (ThorLabs) and filtered by an 850-nm short pass filter (ThorLabs FES850) to remove unwanted radiation in the emission range. The excitation spot was a circle with a diameter of approximately 6 cm. The output excitation power was ~ 6 W, leading to power density of approximately 0.2 W/cm<sup>2</sup>. Emitted light was passed through a 1,100-nm long pass filter (ThorLabs FEL1100) and focused onto the detector by a lens pair consisting of two NIR achromats (200 and 75 mm; Thorlabs). The camera was set to expose continuously with an exposure time of 100 ms and images were acquired with a frame rate of 8.4 frame/sec due to a 19 ms overhead in the readout. 1800 consecutive frames were collected, leading to a total imaging time of 214.2 s. Four BALB/c mice were used, and results shown are representative.

### Post-injection NIR imaging

Mice (n=4) injected with 200 µL of 0.35 mg/mL C<sub>18</sub>-PMH-mPEG (90 kDa) coated SWNT suspension were imaged at 6 h, 24 h, 48 h and 72 h post injection. The same 808 nm laser excitation cleaned by 850-nm short pass filter and 2D InGaAs camera equipped with 1100-nm long pass filter were used as in the video-rate imaging. An exposure time of 300 ms was used to take still images of fluorescence in the 1.1~1.4 µm NIR region. Representative NIR fluorescence images on the same mouse were shown after flat field correction for any non-uniformity of excitation beam.

### Ex Vivo Biodistribution and Circulation

4–8 µl of blood was collected from the tail artery of the mice (n=4) at various time points after injection of 200 µL of 0.35 mg/mL C<sub>18</sub>-PMH-mPEG (90 kDa) coated SWNTs. 8 µl of tissue lysis buffer was added to each blood sample. The samples were bath sonicated for 30 seconds to create a homogenous solution. Using a 785 nm laser diode as the excitation source, the Raman scattering spectrum from the solution was collected. The area under the SWNT graphitic 'G' peak was integrated after background subtraction. This was done 3 times for each sample to get an average value from which the % Injected Dose/gram tissue could be calculated after normalization to the 'G' peak area for the injected solution.

100 hours after injection of SWNT solution, the mice (n=4) were sacrificed and organs were collected in individual vials and weighed. A 2 % sodium cholate solution in 1 mL of Solvable© was added to each vial, followed by heating at 70 °C for two hours to dissolve the organs and create a homogenous solution. The same protocol for circulation was used for collecting the Raman and determining the % ID/gram of the organs.

For characterization of DSPE-mPEG SWNT biodistribution and circulation, the same protocol as above was used on three mice.

### Tumor slice staining

For one of the tumor bearing mice, after 200  $\mu\text{L}$  of 0.35 mg/mL  $\text{C}_{18}$ -PMH-mPEG (90 kDa) coated SWNT solution was intravenously injected, the mouse was sacrificed 100 hours after injection and the tumor was dissected and immediately placed in Optimal Cutting Temperature (OCT) compound, frozen with liquid nitrogen, and stored at  $-80^\circ\text{C}$ . Using a Heidelberg microtome, 40  $\mu\text{M}$  thick slices of the tumor were collected and placed on superfrost plus glass substrates, 45 slices in total, leading a total thickness of 1.8 mm for the tumor. The tumor slices were soaked in cold acetone for 10 minutes, washed three times by 1 $\times$  PBS and then incubated in protein block (3% FBS in 1 $\times$  PBS Tween) overnight at  $4^\circ\text{C}$ . Following a wash by 1 $\times$  PBS-Tween (0.05%), 0.039  $\mu\text{g}/\text{mL}$  (300 pM) rat anti-mouse CD31 (BD Pharmingen) was incubated with the slices in a 10% FBS/80% 1 $\times$ PBS/10% 1 $\times$ PBS-Tween(0.05%) solution for 3 hours. The tumor slices were then washed twice with 1 $\times$ PBS-Tween (0.05%) and incubated with Cy5-labeled anti-rat IgG (H+L) antibody (Jackson Immuno research).

### Tumor slice imaging and 3D reconstruction

To determine the location of SWNTs in each tumor slice, a 658 nm laser diode cleaned by 750 nm short pass filter (Thorlabs) with an 800  $\mu\text{m}$  diameter spot was focused by a 10 $\times$  objective lens (Bausch + Lomb). The resulting CNT fluorescence was collected using a 2D InGaAs camera (Princeton Instruments) equipped with an 1100 nm long-pass filter (Thorlabs) at an exposure time of 300 ms. Due to the larger size of each tumor slice than the field of view, the 10 $\times$  objective block-scanned the whole slice with a step size of 426  $\mu\text{m}$  in  $x$  and 518  $\mu\text{m}$  in  $y$ , leading to each block of 426  $\mu\text{m} \times 518 \mu\text{m}$ . LabVIEW was used to control the block-scanning as well as to stitch all images to form a large image. To image Cy5-labeled anti-mouse CD31 in each tumor slice, the same 658 nm laser diode cleaned by a 655 nm (40 nm bandwidth) bandpass filter (Semrock) with an 800  $\mu\text{m}$  diameter spot was focused by a 10 $\times$  objective lens (Bausch + Lomb). The resulting CNT fluorescence was collected using a Si CCD camera (Hamamatsu) equipped with a 716 nm (40 nm bandwidth) bandpass filter (Semrock) at an exposure time of 100 ms. Due to the larger size of each tumor slice than the field of view, the 10 $\times$  objective block-scanned the whole slice with a step size of 280  $\mu\text{m}$  in  $x$  and 360  $\mu\text{m}$  in  $y$ , leading to each block of 280  $\mu\text{m} \times 360 \mu\text{m}$ . LabVIEW was used to control the block-scanning as well as to stitch all images to form a large image. Matlab 7 was used to color-code SWNT fluorescence in red and Cy5 in green and to overlay the two channels. ImageJ was then used to reconstruct the 3D image based on all 45 slice images.

### SWNT *in vitro* toxicity assay

A MTS colorimetric assay kit, CellTiter96 (Promega), was used to determine the 90 kDa  $\text{C}_{18}$ -PMH-mPEG SWNT cytotoxicity *in vitro*. 4T1 murine breast cancer cells (ATCC #: CRL-2539) were added to a 96 well plate (7500 cells/well) and incubated with 100  $\mu\text{l}$  of 1640 RPMI medium and serially diluted SWNTs ( $n=4$ ). Cells were incubated for 24 hours at 5%  $\text{CO}_2$  and  $37^\circ\text{C}$ . Afterwards, the SWNTs and old medium were replaced with fresh medium and 15  $\mu\text{l}$  of CellTiter96. Initial absorbance readings were taken for each well. After 1 additional hour of incubation, absorbance readings were taken again and the absorbance change was correlated to cell viability.

### Supplementary Material

Refer to Web version on PubMed Central for supplementary material.



## Acknowledgments

This work was supported by the National Institute of Health (NIH-NCI) (grant number 5R01A135109-02).

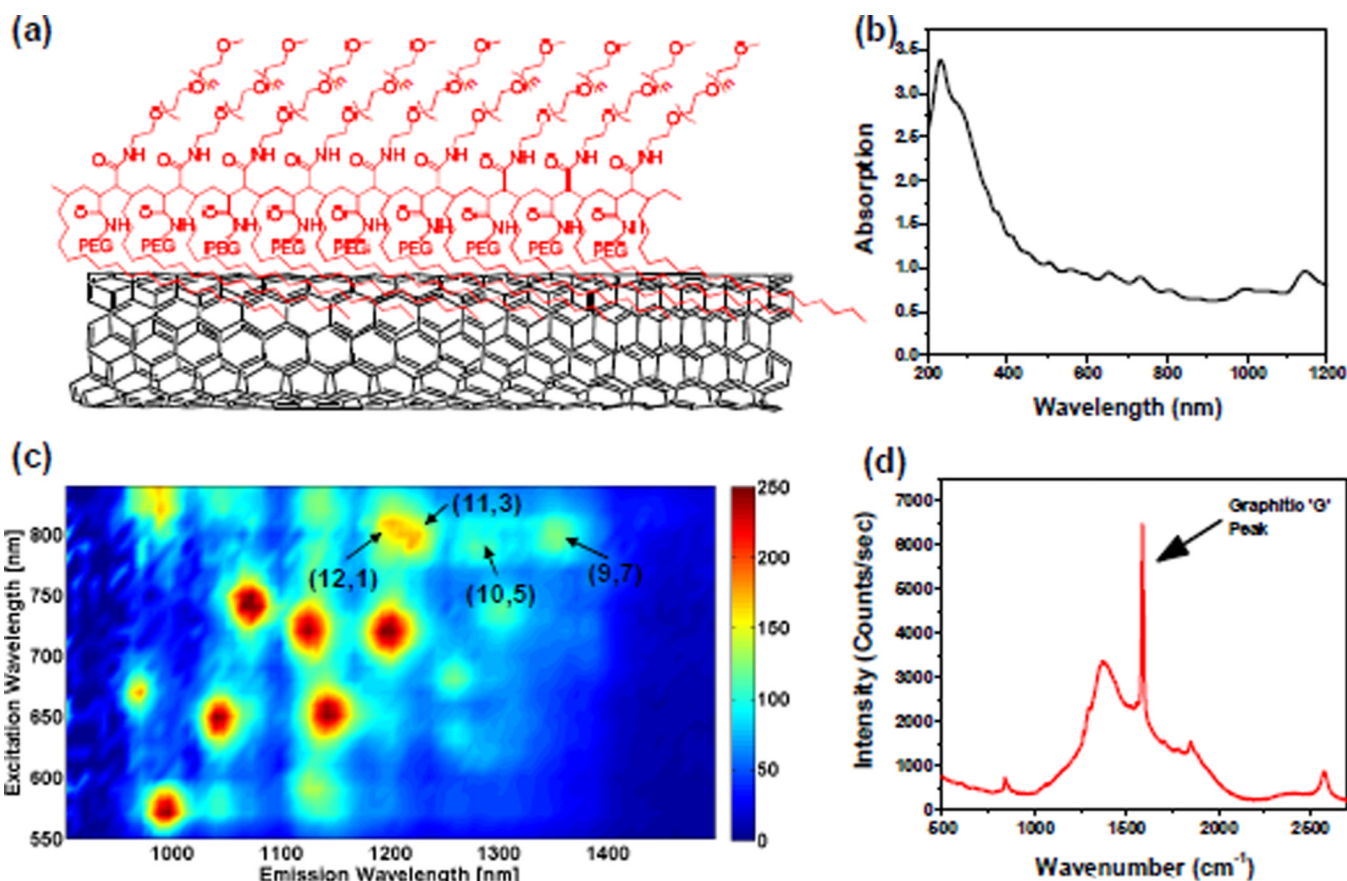
## ABBREVIATIONS

<b>SWNT</b>	Single-walled Carbon Nanotube
<b>PCA</b>	Principal Component Analysis

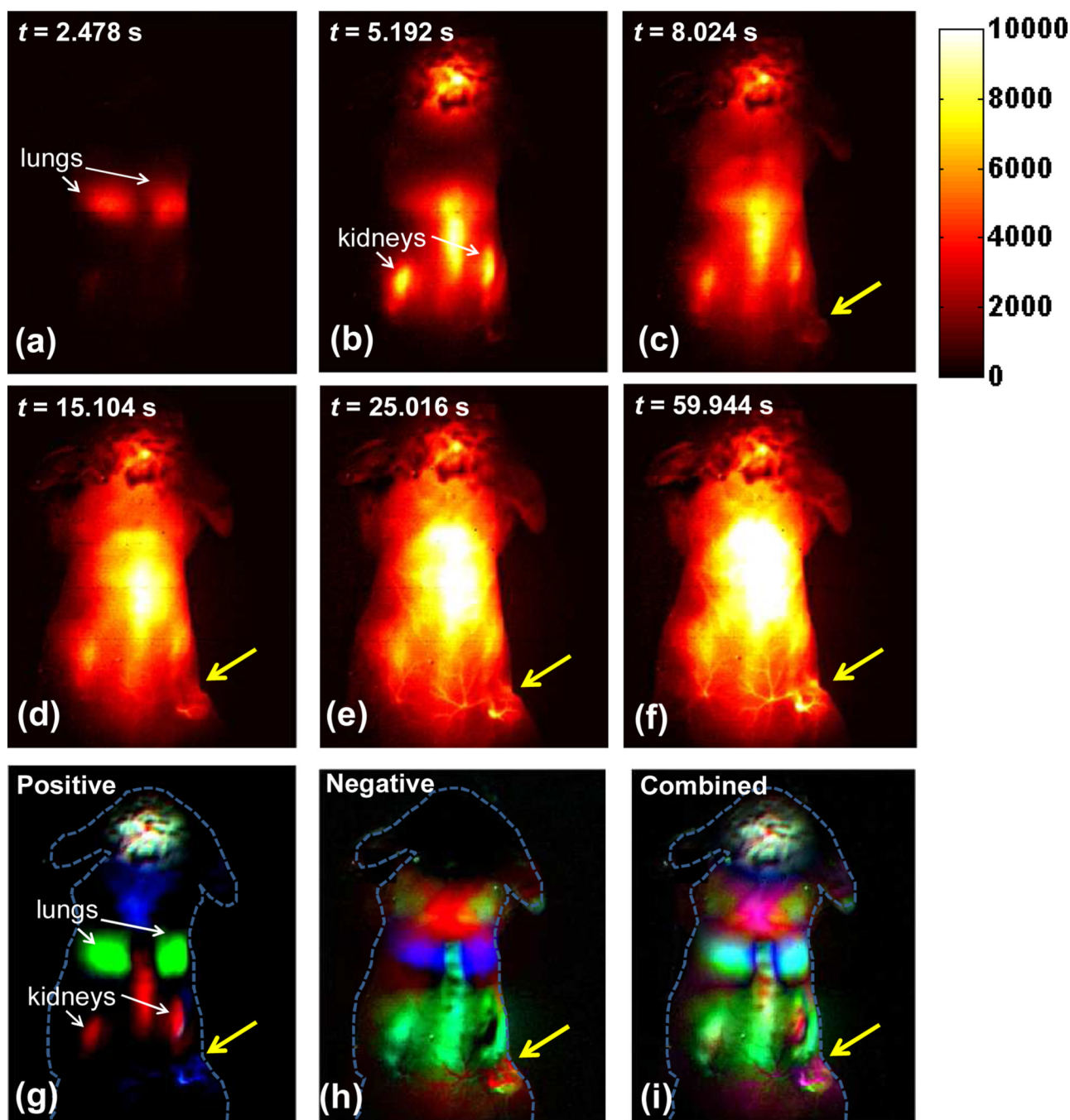
## REFERENCES

1. Wagner V, Dullaart A, Bock AK, Zweck A. *Nature Biotechnol.* 2006; 24:1211–1217. [PubMed: 17033654]
2. Jain RK, Stylianopoulos T. *Nature Rev. Clin. Oncol.* 2010; 7:653–664. [PubMed: 20838415]
3. Stroh M, Zimmer JP, Duda DG, Levchenko TS, Cohen KS, Brown EB, Scadden DT, Torchilin VP, Bawendi MG, Fukumura D, Jain RK. *Nature Med.* 2005; 11:678–682. [PubMed: 15880117]
4. Allen PM, Liu W, Chauhan VP, Lee J, Ting AY, Fukumura D, Jain RK, Bawendi MG. *J. Am. Chem. Soc.* 2009; 132:470–471. [PubMed: 20025222]
5. Duncan R. *Nature Rev. Cancer.* 2006; 6:688–701. [PubMed: 16900224]
6. Lim YT, Kim S, Nakayama A, Stott NE, Bawendi MG, Frangioni JV. *Mol. Imaging.* 2003; 2:50–64. [PubMed: 12926237]
7. Terentyuk GS, Maslyakova GN, Suleymanova LV, Khlebtsov NG, Khlebtsov BN, Akchurin GG, Maksimova IL, Tuchin VV. *J. Biomed. Opt.* 2009; 14 021016.
8. Smith AM, Mancini MC, Nie S. *Nature Nanotechnol.* 2009; 4:710–711. [PubMed: 19898521]
9. Welsher K, Liu Z, Sherlock SP, Robinson JT, Chen Z, Daranciang D, Dai H. *Nature Nanotechnol.* 2009; 4:773–780. [PubMed: 19893526]
10. Frangioni JV. *Curr. Opin. Chem. Biol.* 2003; 7:626–634. [PubMed: 14580568]
11. Welsher K, Sherlock SP, Dai H. *Proc. Natl. Acad. Sci. U. S. A.* 2011; 108:8943–8948. [PubMed: 21576494]
12. Lakowicz JR. *Subcell. Biochem.* 1988; 13:89–126. [PubMed: 2577864]
13. Gordon R, Herman GT. *International Review of Cytology—a Survey of Cell Biology.* 1974; 38:111–151.
14. Maeda H, Wu J, Sawa T, Matsumura Y, Hori K. *J. Control.Release.* 2000; 65:271–284. [PubMed: 10699287]
15. Liu Z, Chen K, Davis C, Sherlock SP, Cao Q, Chen X, Dai H. *Cancer Res.* 2008; 68:6652–6660. [PubMed: 18701489]
16. Prencipe G, Tabakman SM, Welsher K, Liu Z, Goodwin AP, Zhang L, Henry J, Dai H. *J. Am. Chem. Soc.* 2009; 131:4783–4787. [PubMed: 19173646]
17. Robinson JT, Welsher K, Tabakman SM, Sherlock SP, Wang HL, Luong R, Dai H. *Nano Res.* 2010; 3:779–793. [PubMed: 21804931]
18. Liu Z, Robinson JT, Tabakman SM, Yang K, Dai H. *Mater. Today.* 2011; 14:316–323.
19. De La Zerda A, Zavaleta C, Keren S, Vaithilingam S, Bodapati S, Liu Z, Levi J, Smith BR, Ma TJ, Oralkan O, Cheng Z, Chen X, Dai H, Khuri-Yakub BT, Gambhir SS. *Nature Nanotechnol.* 2008; 3:557–562. [PubMed: 18772918]
20. De La Zerda A, Liu Z, Bodapati S, Teed R, Vaithilingam S, Khuri-Yakub BT, Chen X, Dai H, Gambhir SS. *Nano Lett.* 2010; 10:2168–2172. [PubMed: 20499887]
21. Welsher K, Liu Z, Daranciang D, Dai H. *Nano Lett.* 2008; 8:586–590. [PubMed: 18197719]
22. Liu X, Tao H, Yang K, Zhang S, Lee ST, Liu Z. *Biomaterials.* 2010; 32:144–151.
23. Matsumura Y, Maeda H. *Cancer Res.* 1986; 46:6387–6392. [PubMed: 2946403]
24. Iyer AK, Khaled G, Fang J, Maeda H. *Drug Discovery Today.* 2006; 11:812–818. [PubMed: 16935749]

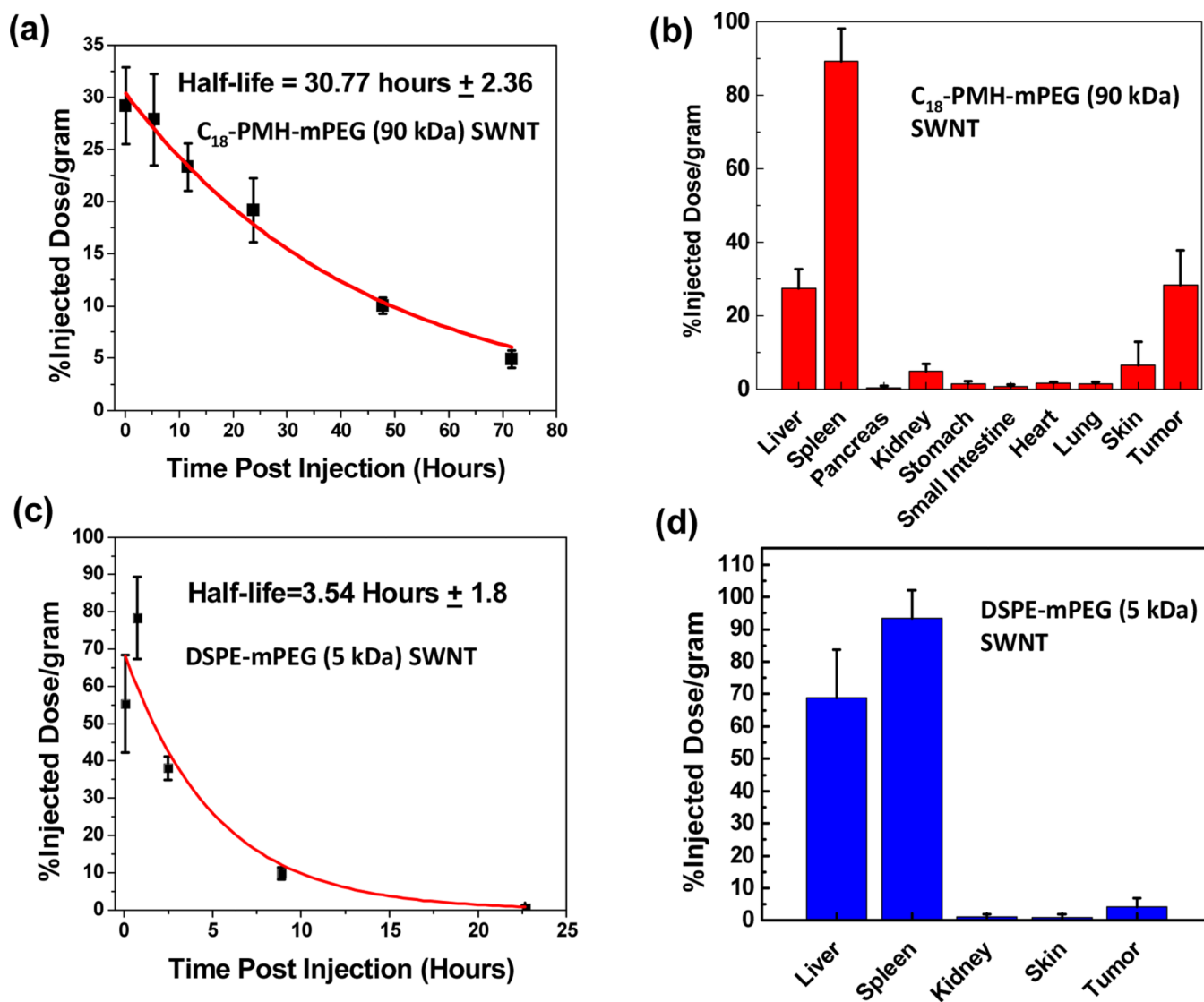
25. Robinson JT, Tabakman SM, Liang Y, Wang HL, Sanchez Casalongue H, Vinh D, Dai H. *J. Am. Chem. Soc.* 2011; 133:6825–6831. [PubMed: 21476500]
26. Liu Z, Tabakman SM, Welsher K, Dai H. *Nano Res.* 2009; 2:85–120. [PubMed: 20174481]
27. Tagmatarchis N, Prato M. *J. Mater. Chem.* 2004; 14:437–439.
28. Prato M, Kostarelos K, Bianco A. *Acc. Chem. Res.* 2008; 41:60–68. [PubMed: 17867649]
29. Hillman EMC, Moore A. *Nature Photonics.* 2007; 1:526–530. [PubMed: 18974848]
30. Folkman J. *Semin. Cancer Biol.* 1992; 3:65–71. [PubMed: 1378311]
31. Shirinifard A, Gens JS, Zaitlen BL, Popławski NJ, Swat M, Glazier JA. *PLoS One.* 2009; 4:e7190. [PubMed: 19834621]
32. Gao XH, Cui YY, Levenson RM, Chung LWK, Nie S. *Nature Biotechnol.* 2004; 22:969–976. [PubMed: 15258594]
33. Liu Z, Davis C, Cai W, He L, Chen X, Dai H. *Proc. Natl. Acad. Sci. U.S.A.* 2008; 105:1410–1415. [PubMed: 18230737]
34. Liu Z, Cai W, He L, Nakayama N, Chen K, Sun X, Chen X, Dai H. *Nature Nanotechnol.* 2007; 2:47–52. [PubMed: 18654207]
35. Bagalkot, V.; Kyung Yu, M.; Jon, S. *Nanoplatform-Based Molecular Imaging.* John Wiley & Sons, Inc.; 2011. p. 565-592.
36. Wong C, Stylianopoulos T, Cui J, Martin J, Chauhan VP, Jiang W, Popovi Z, Jain RK, Bawendi MG, Fukumura D. *Proc. Natl. Acad. Sci. U. S. A.* 2011; 108:2426–2431. [PubMed: 21245339]
37. Giatromanolaki A, Koukourakis MI, Theodossiou D, Barbatis K, O'Byrne K, Harris AL, Gatter KC. *Clin. Cancer Res.* 1997; 3:2485–2492. [PubMed: 9815651]



**Figure 1.** Characterization of  $C_{18}$ -PMH-mPEG (90 kDa) coated SWNTs. (a) A schematic of the water soluble SWNT conjugate (b) A UV-Vis-NIR absorption spectrum of the suspension (c) A 2D photo-excitation and emission (PLE) map of a  $C_{18}$ -PMH-mPEG (90 kDa) coated SWNTs, with different chirality SWNTs showing up as bright spots. (d) A Raman scattering spectrum of the SWNT suspension excited by a 785 nm laser. The graphitic band (G band) is indicated by an arrow at  $\sim 1600\text{ cm}^{-1}$ .



**Figure 2.** Time course NIR-II fluorescence images and dynamic contrast-enhanced images based on PCA analysis. (a–f) NIR-II fluorescence images of a 4T1 tumor bearing mouse after injection of a 200  $\mu\text{L}$  solution containing 0.35 mg/mL SWNTs. (g) Positive pixels from PCA, showing lungs, kidneys and major vessels in the tumor (h) Negative pixels from PCA, showing the body of the tumor. (i) Overlaid image showing the absolute value of both positive and negative pixels, from which both the vessels in the tumor and the tumor outline can be seen. Yellow arrows in images highlight the tumor.

**Figure 3.**

a) Concentration of SWNTs (black symbols) in blood vs. time measured for an injected 90 kDa C<sub>18</sub>-PMH-mPEG SWNT solution (see Methods section). A first order exponential decay model was used for fitting (red curve). b) Biodistribution of the 90 kDa C<sub>18</sub>-PMH-mPEG SWNTs in various organs measured by collecting organs from the mice (n=4) 100 hours after injection (see Methods). c) Circulation and d) biodistribution of DSPE-mPEG (5 kDa) coated SWNT *in vivo* (n=3).

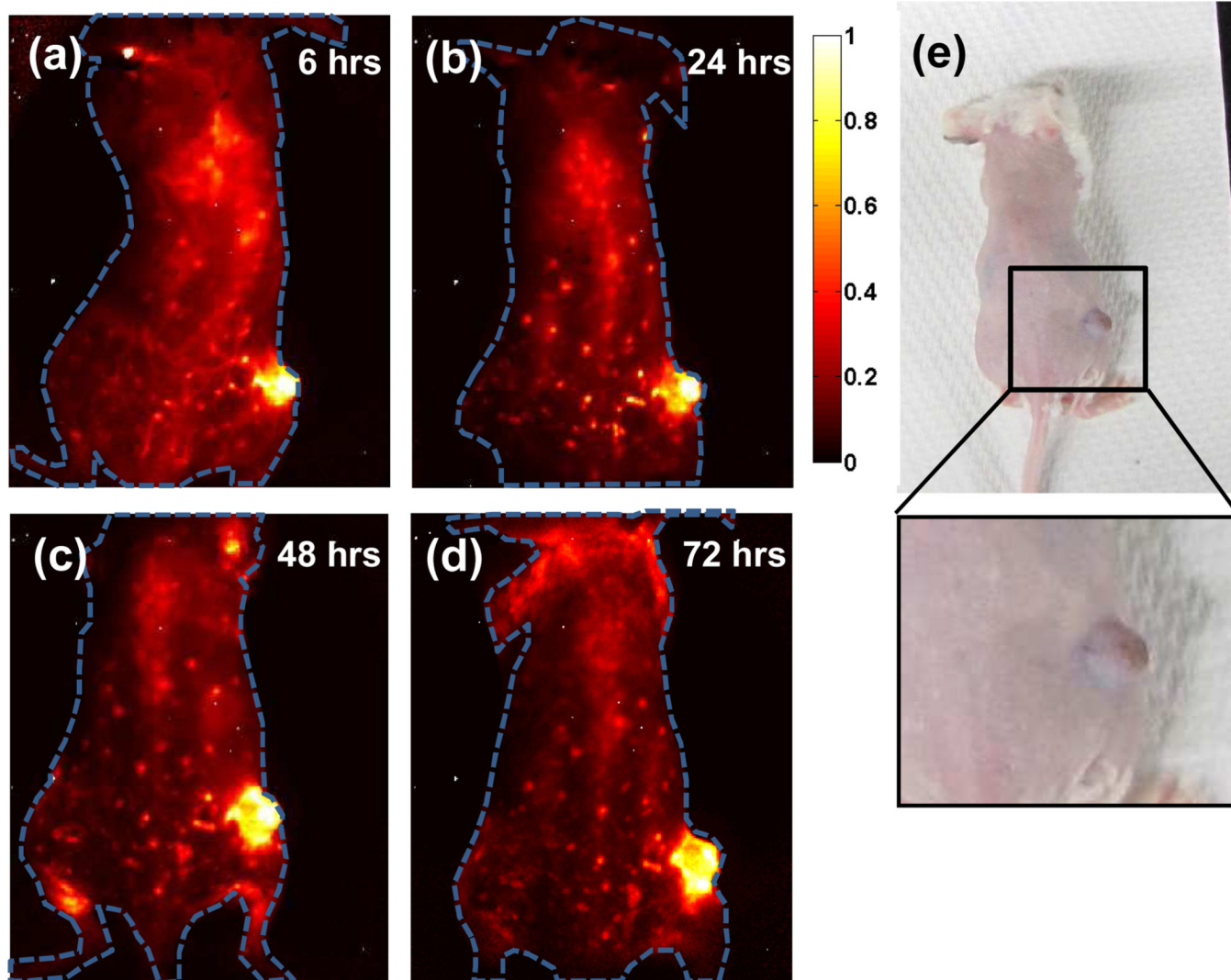


**Figure 4.** NIR-II imaging of xenograft 4T1 tumor with high uptake of SWNTs (a–d) Time course NIR-II fluorescence images of the same mouse injected with  $C_{18}$ -PMH-mPEG (90 kDa) coated SWNTs, showing increasing tumor contrast due to the accumulation of nanotubes inside the tumor. (e) A digital camera image of the same mouse as shown in 4a–d, with noticeable darkening of the tumor due to the high tumor uptake of SWNTs.

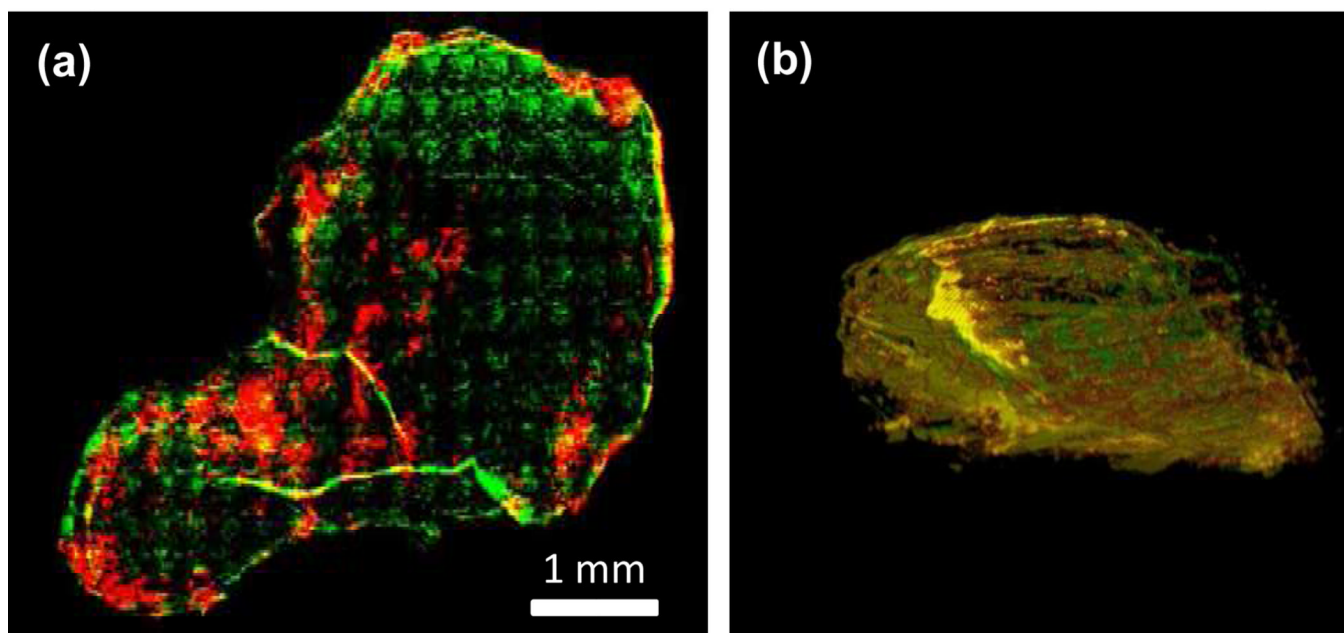


**Figure 5.**

*Ex vivo* imaging of 4T1 murine tumor slices with high SWNT uptake. (a) A tumor slice from a tumor showing the location of SWNTs (coded in red) and Cy5-labeled anti-mouse CD31 (coded in green), and their colocalization (yellow). (b) A reconstructed 3D snapshot image taken from Supplementary Movie 2 with the same color coding as in (a).